A. Parrinello, G.L. Ghiringhelli
Transfer Matrix Representation for Periodic Planar Media
Journal of Sound and Vibration, Vol. 371, 2016, p. 196-209
doi:10.1016/j.jsv.2016.02.005

Transfer Matrix Representation for Periodic Planar Media

A. Parrinello*, G. L. Ghiringhelli

Dipartimento di Scienze e Tecnologie Aerospaziali, Politecnico di Milano
Via La Masa 34, 20156 Milano, Italy

Abstract

Sound transmission through infinite planar media characterized by in-plane periodicity is faced by exploiting the free wave propagation on the related unit cells. An appropriate through-thickness transfer matrix, relating a proper set of variables describing the acoustic field at the two external surfaces of the medium, is derived by manipulating the dynamic stiffness matrix related to a finite element model of the unit cell. The adoption of finite element models avoids analytical modeling or the simplification on geometry or materials. The obtained matrix is then used in a transfer matrix method context, making it possible to combine the periodic medium with layers of different nature and to treat both hard-wall and semi-infinite fluid termination conditions. A finite sequence of identical sub-layers through the thickness of the medium can be handled within the transfer matrix method, significantly decreasing the computational burden. Transfer matrices obtained by means of the proposed method are compared with analytical or equivalent models, in terms

*Corresponding author
Email addresses: andrea.parrinello@polimi.it (A. Parrinello), gianluca.ghiringhelli@polimi.it (G. L. Ghiringhelli)

of sound transmission through barriers of different nature.

Keywords: FEM, Periodic Media, Transfer Matrix, Sound Transmission

1. Introduction

The design of sound barriers is of utmost importance in many applications including automotive, aerospace and buildings. Multi-layer panels are commonly used as wall partitions, airplane flooring and cabin structures and sound transmission through these components has great relevance. Sound transmission through panels can be evaluated experimentally [1], numerically or analytically. Since an alternative numerical approach is proposed here, a brief overview of the most common numerical methods is presented in the following.

Models based on well-known numerical methods, such as the Finite Element Method (FEM) [2, 3, 4, 5] and the Boundary Element Method (BEM) [6], can provide an accurate computation of sound transmission. However, they require extensive computing resources and are inappropriate for large structures and high frequency calculation, when the vibration wavelength becomes much smaller than the structural dimensions.

Statistical Energy Analysis (SEA) [7, 8] has also proven to be a useful tool in the task of predicting sound transmission through partitions. SEA is appropriate for high frequency calculation but is known to fail at low frequencies where the number of modal resonance frequencies in the analysis band is low. The SEA methodology can be exploited either with a *modal approach*, *i.e.* by modeling each subsystem as a superposition of the resonant responses, or with a *wave approach*, *i.e.* by modeling each subsystem as a superposition

of waves traveling through the structure. The latter way consists in deriving and solving a dispersion set of equations between wavenumbers and frequencies for the subsystem of interest. Modal density, group and phase velocities, radiation efficiency and loss-factor are calculated using dispersion relations solutions. These quantities can be evaluated over many kinds of structures, *e.g.* for waveguides [9], curved laminates and composite sandwich panels [10]. The combination of a wave approach with the finite element (FE) model of a unit cell leads to the dispersion problem of the related periodic structure [11, 12]. Vibroacoustic responses of various periodic structures are presented in [13] and [14]. The mathematics of wave propagation in periodic systems has been discussed by Brillouin [15] in the field of electrical engineering. Cremer and Leilich [16] and Heckl [17] investigate on periodic structures formed by assemblages of beams and plates. The effect of damping, the nature of propagation waves and their possible interaction with acoustic waves have been discussed by Mead [18, 19]. In all the papers referred to, exact, harmonic solutions have been found for the equations of motion of the periodic system. Mead [20] and Abrahamson [21] have involved the Rayleigh-Ritz technique in order to treat non-uniform periodic structures. Afterwards, Orris and Petyt [22, 23] have employed the FE technique for wave propagation analysis.

An alternative approach is the Transfer Matrix Method [24] (TMM). Matrix representation of sound propagation is an efficient and largely used tool for modeling plane acoustic fields in stratified media. The problem is formulated in the frequency domain. The layers are assumed to be laterally infinite, and can be of different natures. Nonetheless, at low frequencies, where the

effects of size are important, it is essential to include appropriate corrections, accounting for the finite radiating area. An approach, to the specific problem of airborne transmission losses, is based on application of the spatial windowing technique [10, 25, 26]. Analytical expressions for the transfer matrices are only available for elastic solids, thin plates, fluids and poro-elastic media. On the basis of the three-dimensional (3D) elasticity theory, Huang and Nutt [27] derive the transfer matrix of a general anisotropic layer. Description of non-homogeneous structures is difficult, *e.g.* honeycomb panels, ribbed panels, stud based double-leaf walls, panels with PZT patches and viscoelastic inclusions or functionally graded components in general. An equivalent homogeneous representation can be derived for some heterogeneous structures, such as for honeycomb panels. For other structures, homogenization may be ineffective. Moreover, significant contributions to the dynamic behavior could be lost in homogenization, especially local high-frequency dynamics.

The present work aims to extend the use of the TMM to more general barriers, *e.g.* the ones above mentioned, by exploiting the features of FE modeling. A procedure is derived to obtain the transfer matrix, related to a specific incident plane wave, for an infinite planar medium characterized by in-plane periodicity. First, a proper 3D unit cell of the periodic medium is modeled by means of FEs and the related dynamic stiffness matrix (DSM) is obtained. Then, this latter is manipulated by applying proper conditions to the periodic boundaries, according to the trace of the incident plane wave. Finally, a further condensation of the DSM, with respect the trace of the incident plane wave, leads to the desired one-dimensional through-thickness model and the related transfer matrix.

The proposed procedure combines the versatility of a FE model and the efficiency of the TMM. The combination of a FE model of the cell with a wave approach accurately describes the dynamics involved in acoustic transmission, and the transfer matrix obtained makes it possible to exploit the ability of the TMM by efficiently combining layers of different natures, leading to simple and effective computation of all the required acoustic indicators. Moreover, matrix representation prevents the troubles associated with dealing with dispersion curves and SEA models, thereby avoiding the need for analyst intervention. Thus, the proposed procedure for evaluating the acoustic properties of a barrier can be termed *direct*, since it implicitly involves the wave dispersion in the medium through the DSM of the related unit cell. In contrast, a procedure which requires the dispersion solution for the wave characterization of the medium could be termed *indirect*. Possible applications of the proposed procedure on heterogeneous media include functionally graded plates [28], 3D braided composite [29], 3D woven composites [30, 31] and stud based double-leaf walls [4, 5].

Section 2 presents an overview of the TMM for the phenomenon of acoustic transmission through flat and infinitely extended media. The transfer matrix of a periodic medium will then be derived in section 3, and a number applications will demonstrate the effectiveness of the proposed procedure in section 4.

2. Transfer Matrix Method

Let us consider a flat, infinitely extended, possibly layered, medium separating two semi-infinite media. The right-hand side of Fig. 1 shows a plane

wave impinging upon the bottom surface of the flat structure at an incidence angle of θ_I with an orientation with respect to the x direction defined by the heading angle α (left hand side of Fig. 1). Both a reflected wave and a transmitted wave will therefore propagate from the interposed medium. Continuity of the velocity at the bottom interface shows that the angles of incidence and reflection are equal: $\theta_I = \theta_R = \theta$. The angle of transmission, θ_T, depends on the propagation through the thickness. For real wavenumbers and thin barriers, Snell's law of refraction states that: $\sin(\theta_I)/c_1 = \sin(\theta_T)/c_2$, where c_1 and c_2 are the phase velocities in the two semi-infinite media. The amplitudes of the reflected and transmitted waves will depend on the inertial and mechanical properties of the barrier. According to their properties, various types of waves can propagate in each layer of the interposed material. Sound transmission through the medium is fully characterized by these waves. The $x-y$ components of the wavenumber of each wave propagating in each layer are equal to the $x-y$ components of the incident wave in the semi-infinite medium, *i.e.*:

$$k_x = \frac{\omega}{c_1}\sin(\theta)\cos(\alpha) \ , \quad k_y = \frac{\omega}{c_1}\sin(\theta)\sin(\alpha) \ . \tag{1}$$

In other words, the incident plane wave produces only plane acoustic fields in the stratified medium, characterized by the same $x-y$ wavenumber components. The acoustic field in a layer is completely defined by the nature of the waves propagating in it and by their amplitudes [24].

2.1. Matrix representation

In a TMM context, each layer is replaced by a matrix linking the values of a proper set of variables at the opposite interfaces. First, the relationship

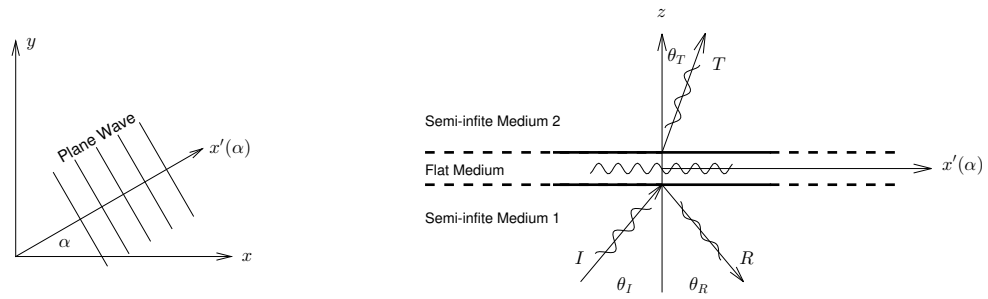

Figure 1: Plane wave reflection and transmission at a plane interface between two semi-infinite media

between a set of variables which describe the acoustic field at a specific height, $\mathbf{V}(z_j)$, and the wave amplitudes vector, $\mathbf{A}_j$, must be defined for the j-th layer through a square matrix: $\mathbf{V}(z_j) = \Gamma(z_j)\mathbf{A}_j$. Finally, the variables at the bottom interface of the layer, $\mathbf{V}_{Bj}$, can be related to the variables at the top interface, $\mathbf{V}_{Tj}$:

$$\mathbf{V}_{Bj} = \Gamma(z_{Bj})\Gamma(z_{Tj})^{-1}\mathbf{V}_{Tj} = \mathbf{T}_j(\omega, \theta, \alpha)\mathbf{V}_{Tj} \ . \tag{2}$$

The transfer matrix thus obtained for a specific incident plane wave, $\mathbf{T}_j(\omega, \theta, \alpha)$, depends on the thickness and physical properties of the layer. Analytical expressions for the transfer matrices of different kind of layers are available in [24].

2.2. Assembling the global transfer matrix

The transfer matrix of a layered medium is obtained from the transfer matrices of individual layers by imposing continuity conditions at interfaces

as

$$\mathbf{H}_0 = \begin{bmatrix} \mathbf{I}_{f1} & \mathbf{J}_{f1}\mathbf{T}_1 & \mathbf{0} & \cdots & \mathbf{0} & \mathbf{0} \\ \mathbf{0} & \mathbf{I}_{12} & \mathbf{J}_{12}\mathbf{T}_2 & \cdots & \mathbf{0} & \mathbf{0} \\ \vdots & \vdots & \vdots & \ddots & \vdots & \vdots \\ \mathbf{0} & \mathbf{0} & \mathbf{0} & \cdots & \mathbf{J}_{(n-2)(n-1)}\mathbf{T}_{n-1} & \mathbf{0} \\ \mathbf{0} & \mathbf{0} & \mathbf{0} & \cdots & \mathbf{I}_{(n-1)(n)} & \mathbf{J}_{(n-1)(n)}\mathbf{T}_n \end{bmatrix} , \quad (3)$$

where $\mathbf{I}_{ij}$ and $\mathbf{J}_{ij}$ are interface matrices which depend on the nature of the i-th and j-th layers and the suffix f denotes the fluid at the excitation side. Details on the interface matrices are fully available in [24]. For a layered medium with n layers of the same nature interface matrices $\mathbf{I}_{ij}$ and $\mathbf{J}_{ij}$ are identity matrices and the global transfer matrix becomes

$$\mathbf{H}_0 = \begin{bmatrix} \mathbf{I}_{f1} & \mathbf{J}_{f1}\mathbf{T} \end{bmatrix} , \quad (4)$$

where

$$\mathbf{T} = \mathbf{T}_1 \cdot \mathbf{T}_2 \cdot ... \cdot \mathbf{T}_n . \quad (5)$$

At the termination side, impedance conditions relating the field variables are needed to well pose the problem. Such conditions closely depend on the nature of the termination: hard wall or semi-infinite fluid. The added equations and variables leads to the matrix $\mathbf{H}$ [24].

2.3. Calculation of the acoustic indicators

For both termination conditions, the impedance condition of the fluid at the excitation side is still needed. Adding this equation to matrix $\mathbf{H}$ allows for the calculation of the acoustic indicators of the problem. The surface impedance of the medium is calculated by

$$Z_s = -\frac{\det \mathbf{H}_1}{\det \mathbf{H}_2} , \quad (6)$$

where $\det \mathbf{H}_i$ is the determinant of the matrix obtained when the i-th column has been removed from $\mathbf{H}$. The reflection coefficient, R, and the absorption coefficient, A, are then given by the classical formulas:

$$R = \frac{Z_s \cos\theta - Z_0}{Z_s \cos\theta + Z_0} \quad \text{and} \quad A = 1 - |R|^2 \ , \tag{7}$$

where Z_0 is the characteristic impedance of the semi-infinite medium. In case of a diffuse field excitation, the absorption coefficient is defined as follows:

$$A_d(\omega) = \frac{\int_0^{2\pi} \int_0^{\theta_{\max}} A(\omega, \theta, \alpha) \cos\theta \sin\theta d\theta d\alpha}{2\pi \int_0^{\theta_{\max}} \cos\theta \sin\theta d\theta} \ . \tag{8}$$

In case of semi-infinite fluid termination, the transmission coefficient, T, and the reflection coefficient, R, are related by

$$\frac{p_1}{1+R} = \frac{p_2}{T} \ , \tag{9}$$

where p_i is the pressure in the i-th semi-infinite fluid, so obtaining

$$T = -(1+R)\frac{\det \mathbf{H}_{N+1}}{\det \mathbf{H}_1} \ . \tag{10}$$

In case of a diffuse field excitation, the transmission loss is defined as:

$$\mathrm{TL}(\omega) = -10 \log \frac{\int_0^{2\pi} \int_0^{\theta_{\max}} |T(\omega, \theta, \alpha)|^2 \cos\theta \sin\theta d\theta d\alpha}{2\pi \int_0^{\theta_{\max}} \cos\theta \sin\theta d\theta} \tag{11}$$

3. Transfer Matrix for Periodic Media

The analytical expression of a transfer matrix can be derived when an analytical wave characterization of the infinitely extended medium is available, as for homogeneous solids, fluids and mixed layers, *e.g.* porous media [24]. On the other hand, deriving the transfer matrix of a heterogeneous medium

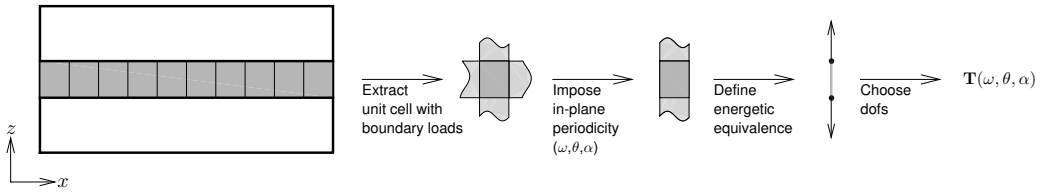

Figure 2: Schematic diagram of the procedure which leads to the transfer matrix, $\mathbf{T}$, of a periodic medium (gray box) bounded by two semi-infinite media (white boxes)

can be difficult or computationally expensive. Thus, a numerical procedure for deriving the transfer matrix of a generic medium with in-plane periodicity starting from the FE model of its unit cell is proposed here. The main steps in the procedure are illustrated in Fig. 2 and discussed below. It should be noted that also a homogeneous medium may be seen as a periodic one with respect to a unit cell with proper shape but arbitrary dimensions. The partitioning of the whole layer in a finite number of identical sub-layers, n, can be handled directly within the TMM according to Eq. (5). The transfer matrix for the 2D periodic sub-layer, $\mathbf{T}_0$, can be obtained with the present procedure and finally the transfer matrix of the layered medium, $\mathbf{T}$, can be derived as

$$\mathbf{T} = \underbrace{\mathbf{T}_0 \cdot \mathbf{T}_0 \cdot \ldots \cdot \mathbf{T}_0}_{n \text{ times}} = \mathbf{T}_0^n \ . \tag{12}$$

3.1. Two-dimensional periodicity conditions

A 2D periodic structure is composed of identical elementary components, or cells, connected to one another to cover a plane. Wave characterization of the periodic medium is the first step in deriving its transfer matrix. Wave motion through the periodic system is analyzed using Bloch's theorem [15], which states that the proportionate change in wave amplitude occurring from

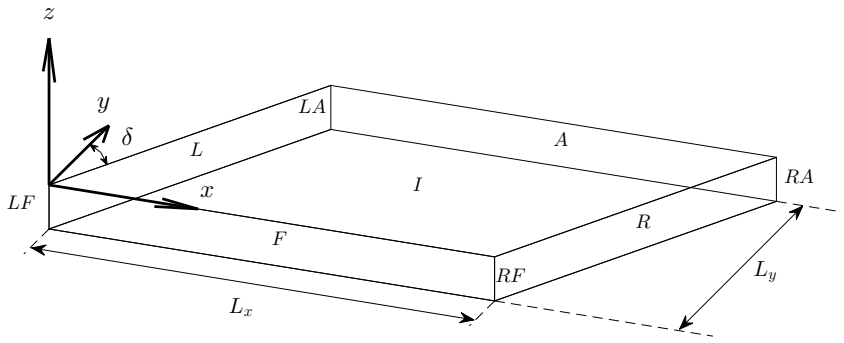

Figure 3: Unit cell of a generic structure periodic in the $x-y$ plane

cell to cell depends on the propagation vector and does not depend on the cell's location within the periodic system. Propagation components are complex numbers whose real and imaginary parts are denoted, respectively, as *attenuation* and *phase* constants. Waves are free to propagate if the propagation constants are purely imaginary, while their amplitude is attenuated if the real part of the propagation constants is non-zero. Since the domain is unbounded in the $x-y$ plane and the input acoustic field is spatially uniform, only free wave propagation (real wavenumbers) will be considered here.

The Bloch's theorem can be combined with an FE model of the structure by adopting the periodic theory developed by Orris and Petyt [22]. Fig. 3 depicts the unit cell, of dimensions L_x and L_y, extracted from an infinitely extended periodic structure. The skew angle, δ, increases the flexibility of the procedure, making it possible to deal with unit cells with the lowest dimensions, *e.g.* the minimal unit cell in a hexagonal honeycomb panel is a right prism with parallelogram bases.

We consider a generic medium with a linear solid phase and a fluid phase.

Figure 4: Planar structures (black) converted into barriers with flat interfaces adding fluid phases (gray)

Such a choice allows to handle layers with mixed interfaces, *e.g.* perforated panels or honeycomb cores, and layers with non-flat interfaces, *e.g.* panels with added patches and corrugated or stiffened panels, that can be considered planar only in a broad sense. Models are available in the TMM context for the first class of structures, while the method seems to be not suitable for the second one. This latter can be treated by adding fluid phases in order to obtain flat interfaces suitable for plane wave excitation; see Fig. 4.

For time harmonic motion at frequency ω, the governing equation of the extracted unit cell is [32]

$$\left(\begin{bmatrix} \mathbf{K}_s & \mathbf{B}^T \\ \mathbf{0} & \mathbf{K}_f \end{bmatrix} + i\omega \begin{bmatrix} \mathbf{C}_s & \mathbf{0} \\ \mathbf{0} & \mathbf{C}_f \end{bmatrix} - \omega^2 \begin{bmatrix} \mathbf{M}_s & \mathbf{0} \\ -\rho_f \mathbf{B} & \mathbf{M}_f/c^2 \end{bmatrix} \right) \begin{Bmatrix} \mathbf{q}_s \\ \mathbf{p} \end{Bmatrix} = \begin{Bmatrix} \mathbf{b}_s \\ \mathbf{b}_f \end{Bmatrix} \quad (13)$$

where the subscripts s and f identify the quantities related to the solid phase and the fluid phase respectively, $\mathbf{K}$, $\mathbf{C}$ and $\mathbf{M}$ are stiffness, damping and mass matrices respectively, $\mathbf{B}$ is the solid-fluid interface matrix, c is the speed of sound in the fluid phase, ρ_f is the fluid density, $\mathbf{q}_s$ and $\mathbf{b}_s$ are the vectors of generalized displacements and forces in the solid phase, the vector $\mathbf{p}$ collects the nodal pressures in the fluid mesh and $\mathbf{b}_f$ is the vector of generalized forces acting on the fluid phase at external boundaries. The medium may have fluid, solid or mixed interfaces. The desired transfer matrix must depend on the physical properties of the layer only. In order to enforce such a condition, a weak coupling between layers must be hypothesized; that is, a particular

Figure 5: Unit cells corresponding to the same periodic medium cut at different vertical planes

load acting on a layer interface can't alter its dynamical properties. Such a hypothesis is deeply linked to the small perturbations assumption of linear acoustics. To exploit the weak coupling hypothesis, the dynamic problem can be rewritten by splitting boundary forces as

$$\mathbf{D}(\omega)\mathbf{q} = \mathbf{f} + \mathbf{e} \ , \tag{14}$$

where $\mathbf{D}(\omega)$ is the dynamic stiffness matrix (DSM), $\mathbf{q}$ is the vector of generalized displacements, including pressures, $\mathbf{f}$ is the vector of generalized internal forces, *i.e.* due to adjacent unit cells, and $\mathbf{e}$ is the vector of generalized external forces, *i.e.* due to bounding media. An internal boundary, *i.e.* related to an adjacent unit cell, may coincide with a physical boundary for the medium, as in the case of the unit cell depicted on the right side of Fig. 5, or it may not, as in the unit cell depicted on the left side. In the latter case the subset $\mathbf{f}_f$ related to the fluid phase equates to a zero vector, since the equilibrium condition between opposite internal boundaries is ensured by the pressure continuity in the fluid. So, the unit cell depicted on the left side of Fig. 5 simplifies the FE model. Anyway, the subset $\mathbf{f}_f$ grants versatility in the definition of the unit cell. Moreover, the subset $\mathbf{e}_f$ equates to a zero vector for layers with solid interfaces.

It is anticipated here that the presence of forces vectors in the dynamic equation, Eq. (14), is only formal. In fact, internal forces will be removed

from the problem through reduction of periodicity, and external forces will remain unknown, since we are interested in the transfer matrix. Only the DSM, $\mathbf{D}(\omega)$, will therefore be involved in the procedure. Extracting the unit cell from the infinitely extended medium, modeling the cell using any FE package and applying external forces represent the operations defining the first step in the procedure illustrated in Fig. 2.

As we have anticipated, the dynamic system must be reduced by linking displacements and forces at opposite boundaries in the $x-y$ plane. In order to apply the required conditions, we distinguish in the unit cell between an internal region (I), the left (L), right (R), after (A) and forward (F) surfaces and four edges (LF,LA,RF,RA); see Fig. 3. Accordingly, the vector of degrees of freedom (DOFs), $\mathbf{q}$, is partitioned as

$$\mathbf{q} = [\mathbf{q}_I \;\; \mathbf{q}_E \;\; \mathbf{q}_A \;\; \mathbf{q}_R \;\; \mathbf{q}_{RF} \;\; \mathbf{q}_{LA} \;\; \mathbf{q}_{RA}]^T \quad \text{with} \quad \mathbf{q}_E = [\mathbf{q}_F \;\; \mathbf{q}_L \;\; \mathbf{q}_{LF}]^T . \tag{15}$$

The vector of internal forces, $\mathbf{f}$, is partitioned in the same manner

$$\mathbf{f} = [\mathbf{0} \;\; \mathbf{f}_E \;\; \mathbf{f}_A \;\; \mathbf{f}_R \;\; \mathbf{f}_{RF} \;\; \mathbf{f}_{LA} \;\; \mathbf{f}_{RA}]^T \quad \text{with} \quad \mathbf{f}_E = [\mathbf{f}_F \;\; \mathbf{f}_L \;\; \mathbf{f}_{LF}]^T , \tag{16}$$

where the partition for the internal region, $\mathbf{f}_I$, has been replaced with a zero vector. The vector of external forces, $\mathbf{e}$, is not involved in this partitioning. In order to simplify the following exposure, we suppose that the nodes at opposite boundaries are identically arranged. The procedure could be generalized using interpolation matrices linking generalized displacements and forces at opposite boundaries. Applying Bloch's theorem to the generalized displacements at the boundaries, we obtain the following relations:

$$\mathbf{q}_A = \mathbf{q}_F\lambda_y \;,\; \mathbf{q}_R = \mathbf{q}_L\lambda_x \;,\; \mathbf{q}_{RF} = \mathbf{q}_{LF}\lambda_x \;,\; \mathbf{q}_{LA} = \mathbf{q}_{LF}\lambda_y \;,\; \mathbf{q}_{RA} = \mathbf{q}_{LF}\lambda_x\lambda_y \;, \tag{17}$$

with

$$\lambda_x = \exp(-ik_x L_x) \quad , \quad \lambda_y = \exp(-ik_y L_y \cos(\delta)) \cdot \exp(-ik_x L_x \sin(\delta)) \ , \quad (18)$$

where k_x and k_y are defined by the compatibility relations with respect to the acoustic input, Eq. (1). As a consequence, periodicity conditions depend on the specific incident plane wave. It should be noted that the displacement relations, Eq. (17), also apply to the pressures contained in the vectors. So, by applying Bloch's theorem to the generalized forces at the boundaries and taking into account equilibrium conditions, we obtain the following relations:

$$\mathbf{f}_A = -\mathbf{f}_F \lambda_y \ , \ \mathbf{f}_R = -\mathbf{f}_L \lambda_x \ , \ \mathbf{f}_{RF} = -\mathbf{f}_{LF} \lambda_x \ , \ \mathbf{f}_{LA} = -\mathbf{f}_{LF} \lambda_y \ , \ \mathbf{f}_{RA} = -\mathbf{f}_{LF} \lambda_x \lambda_y \ . \quad (19)$$

Clearly, the assumption of weak coupling between layers prevents periodicity from being affected by external forces, $\mathbf{e}$. Using the periodicity relations, Eqs. (17) and (19), we can express the generalized displacements vector, $\mathbf{q}$, and the generalized internal forces vector, $\mathbf{f}$, as

$$\mathbf{q} = \begin{bmatrix} \mathbf{I} & \\ \mathbf{0} & +\Lambda \end{bmatrix} \begin{Bmatrix} \mathbf{q}_I \\ \mathbf{q}_E \end{Bmatrix} = \mathbf{A}\mathbf{q}' \quad \text{and} \quad \mathbf{f} = \begin{bmatrix} \mathbf{I} & \\ \mathbf{0} & -\Lambda \end{bmatrix} \begin{Bmatrix} \mathbf{0} \\ \mathbf{f}_E \end{Bmatrix} = \hat{\mathbf{A}}\mathbf{f}' \quad (20)$$

with

$$\Lambda = \begin{bmatrix} \mathbf{I}\lambda_y & \mathbf{0} & \mathbf{0} \\ \mathbf{0} & \mathbf{I}\lambda_x & \mathbf{0} \\ \mathbf{0} & \mathbf{0} & \mathbf{I}\lambda_x \\ \mathbf{0} & \mathbf{0} & \mathbf{I}\lambda_y \\ \mathbf{0} & \mathbf{0} & \mathbf{I}\lambda_x\lambda_y \end{bmatrix} \ , \quad (21)$$

where $\mathbf{A}$, $\hat{\mathbf{A}}$ and Λ are complex matrices. The equation of motion, Eq. (14), can be reduced as

$$\mathbf{A}^H \mathbf{D}(\omega) \mathbf{A}\mathbf{q}' = \mathbf{A}^H (\mathbf{f} + \mathbf{e}) \ . \quad (22)$$

Under the assumption of real wavenumbers ($\lambda_x^H = 1/\lambda_x$, $\lambda_y^H = 1/\lambda_y$), we obtain

$$\mathbf{A}^H\mathbf{f} = \mathbf{A}^H\hat{\mathbf{A}}\mathbf{f}' = \begin{bmatrix} \mathbf{I} & \mathbf{0} \\ \mathbf{0} & \mathbf{0} \end{bmatrix} \begin{Bmatrix} \mathbf{0} \\ \mathbf{f}_E \end{Bmatrix} = \mathbf{0} \ . \tag{23}$$

As a consequence, the forces due to neighboring cells disappear from the reduced dynamic problem and we obtain

$$\mathbf{D}'(\omega, \theta, \alpha)\mathbf{q}' = \mathbf{A}^H\mathbf{e} = \mathbf{e}' \ . \tag{24}$$

Applying periodicity conditions to obtain a reduced problem represents the second step in the procedure illustrated in Fig. 2. It should be noted that solving the homogeneous counterpart of the reduced dynamic problem, Eq. (24), for the frequency ω as a function of the propagation constants λ_x and λ_y, yields the frequencies of free wave propagation, *i.e.* the dispersion relations for the periodic medium. Even if the dispersion problem is not solved, all the dispersion information are implicitly involved in the method, since these are contained in the reduced DSM, $\mathbf{D}'(\omega, \theta, \alpha)$. In this sense, the proposed procedure may be termed *direct*, since the solution of the dispersion problem is bypassed.

3.2. Energetic equivalence to one-dimensional through-thickness problem

For a given incident wave, defined by its angular frequency, ω, incident angle, θ, and heading angle, α, its wavenumber components, k_x and k_y, can be computed with Eq. (1) and the reduced problem, Eq. (24), can be derived. The next step in the proposed procedure involves reducing the obtained 3D model to an energetically equivalent 1D model through thickness. In a TMM context, we are interested in representing the energy flow through the components. Since it occurs through the thickness of the layers, we have to

partition the reduced vectors of DOFs, $\mathbf{q}'$, and of external forces, $\mathbf{e}'$, in the top (T), bottom (B) and internal (I) sets. With a view to exploiting the transfer matrix thus obtained in a TMM context, external rotational DOFs and moments must be assigned to internal sets, since rotations at interfaces are not involved in the classic TMM. Thus, rotations are assumed not to be restrained at the interfaces. As a consequence, vectors $\mathbf{q}'_B$ and $\mathbf{q}'_T$ collect displacements and, eventually, pressures regardless of the finite elements used. Moreover, the set of internal forces, $\mathbf{e}'_I$, equates to a zero vector since no internal forces or external moments are applied. The rearranged problem appears as

$$\begin{bmatrix} \mathbf{D}'_{BB} & \mathbf{D}'_{BI} & \mathbf{D}'_{BT} \\ \mathbf{D}'_{IB} & \mathbf{D}'_{II} & \mathbf{D}'_{IT} \\ \mathbf{D}'_{TB} & \mathbf{D}'_{TI} & \mathbf{D}'_{TT} \end{bmatrix} \begin{Bmatrix} \mathbf{q}'_B \\ \mathbf{q}'_I \\ \mathbf{q}'_T \end{Bmatrix} = \begin{Bmatrix} \mathbf{e}'_B \\ \mathbf{0} \\ \mathbf{e}'_T \end{Bmatrix} . \tag{25}$$

The internal dofs set, $\mathbf{q}'_I$, may be eliminated, obtaining the following form

$$\begin{bmatrix} \mathbf{D}'_{BB} - \mathbf{D}'_{BI}\mathbf{D}'^{-1}_{II}\mathbf{D}'_{IB} & \mathbf{D}'_{BT} - \mathbf{D}'_{BI}\mathbf{D}'^{-1}_{II}\mathbf{D}'_{IT} \\ \mathbf{D}'_{TB} - \mathbf{D}'_{TI}\mathbf{D}'^{-1}_{II}\mathbf{D}'_{IB} & \mathbf{D}'_{TT} - \mathbf{D}'_{TI}\mathbf{D}'^{-1}_{II}\mathbf{D}'_{IT} \end{bmatrix} \begin{Bmatrix} \mathbf{q}'_B \\ \mathbf{q}'_T \end{Bmatrix} = \mathbf{C}' \begin{Bmatrix} \mathbf{q}'_B \\ \mathbf{q}'_T \end{Bmatrix} = \begin{Bmatrix} \mathbf{e}'_B \\ \mathbf{e}'_T \end{Bmatrix} . \tag{26}$$

In order to simplify the following exposure, we suppose that the vectors are partitioned as

$$\mathbf{q}'_B = \begin{Bmatrix} \mathbf{q}'_{Bx} \\ \mathbf{q}'_{By} \\ \mathbf{q}'_{Bz} \\ \mathbf{p}'_B \end{Bmatrix} \quad , \quad \mathbf{q}'_T = \begin{Bmatrix} \mathbf{q}'_{Tx} \\ \mathbf{q}'_{Ty} \\ \mathbf{q}'_{Tz} \\ \mathbf{p}'_T \end{Bmatrix} \quad , \quad \mathbf{e}'_B = \begin{Bmatrix} \mathbf{e}'_{Bx} \\ \mathbf{e}'_{By} \\ \mathbf{e}'_{Bz} \\ \mathbf{e}'_{Bf} \end{Bmatrix} \quad , \quad \mathbf{e}'_T = \begin{Bmatrix} \mathbf{e}'_{Tx} \\ \mathbf{e}'_{Ty} \\ \mathbf{e}'_{Tz} \\ \mathbf{e}'_{Tf} \end{Bmatrix} . \tag{27}$$

To build the corresponding 1D model, we have to perform an in-plane weighted sum of information preserving the energy flow. We therefore look for generalized forces whose work equates the work done by the nodal forces with respect to the imposed wave motion. We first define a generalized

displacement function which emulates the incident acoustic wave:

$$\zeta(x, y) = \exp(-i(k_x x + k_y y)) \ . \tag{28}$$

Starting with the bottom surface, the total works done by the four sets of bottom nodal forces with respect to wave motion can be expressed as

$$\sum_{j=1}^{n_{Bs}} \zeta(x_{Bsj}, y_{Bsj}) e'_{B\eta j} \ = \hat{e}_{B\eta} \ \ , \ \ \sum_{j=1}^{n_{Bf}} \zeta(x_{Bfj}, y_{Bfj}) e'_{Bfj} \ = \hat{e}_{Bf} \tag{29}$$

where $\eta = x, y, z$, (x_{Bsj}, y_{Bsj}) and (x_{Bfj}, y_{Bfj}) are the coordinates of the j-th node of the solid phase and of the fluid phase respectively, n_{Bs} and n_{Bf} are the number of nodes on the bottom surface for the solid and the fluid phase and $\hat{e}_{B\eta}$ and $\hat{e}_{Bf}$ are generalized forces formally placed at the origin of the axis (o) where wave motion is unitary ($\zeta_o = 1$). Collecting the four generalized forces in the vector $\hat{\mathbf{e}}_B = [\hat{e}_{Bx} \ \ \hat{e}_{By} \ \ \hat{e}_{Bz} \ \ \hat{e}_{Bf}]^T$, we obtain

$$\hat{\mathbf{e}}_B = \begin{bmatrix} \mathbf{I}_3 \otimes \zeta_{Bs} & \mathbf{0} \\ \mathbf{0} & \zeta_{Bf} \end{bmatrix} \mathbf{e}'_B = \mathbf{L}_B \mathbf{e}'_B \ , \tag{30}$$

where ζ_{Bs} and ζ_{Bf} are row vectors collecting the evaluations of the wave function, ζ, at bottom nodes for the solid phase and for the fluid phase respectively, $\mathbf{I}_3$ is the identity matrix of size 3 and $\otimes$ denotes the Kronecker product. Hence, the nodal displacements vector, $\mathbf{q}'_B$, can be expressed in terms of the vector of a generalized displacements, $\hat{\mathbf{q}}_B = [\hat{q}_{Bx} \ \ \hat{q}_{By} \ \ \hat{q}_{Bz} \ \ \hat{p}_B]^T$, by equating the work done by the generalized forces to the work done by the nodal forces:

$$(\hat{\mathbf{e}}_B)^H \hat{\mathbf{q}}_B = (\mathbf{e}'_B)^H \mathbf{q}'_B \quad \rightarrow \quad \mathbf{q}'_B = \mathbf{L}_B^H \hat{\mathbf{q}}_B \ . \tag{31}$$

The vectors of generalized forces and displacements for the top surface, $\hat{\mathbf{e}}_T$ and $\hat{\mathbf{q}}_T$, can be derived in the same manner by obtaining the top reduction

matrix $\mathbf{L}_T$. If the nodes on the bottom and top surfaces are identically arranged, then the top reduction matrix, $\mathbf{L}_T$, equates the bottom reduction matrix, $\mathbf{L}_B$. Exploiting the projection of the nodal forces, Eq. (30), and the expansion of the generalized displacements, Eq. (31), for both the top and bottom surface, the 1D dynamic problem can be derived:

$$\begin{bmatrix} \mathbf{L}_B\mathbf{C}'_{BB}\mathbf{L}_B^H & \mathbf{L}_B\mathbf{C}'_{BT}\mathbf{L}_T^H \\ \mathbf{L}_T\mathbf{C}'_{TB}\mathbf{L}_B^H & \mathbf{L}_T\mathbf{C}'_{TT}\mathbf{L}_T^H \end{bmatrix} \begin{Bmatrix} \hat{\mathbf{q}}_B \\ \hat{\mathbf{q}}_T \end{Bmatrix} = \mathbf{C} \begin{Bmatrix} \hat{\mathbf{q}}_B \\ \hat{\mathbf{q}}_T \end{Bmatrix} = \begin{Bmatrix} \hat{\mathbf{e}}_B \\ \hat{\mathbf{e}}_T \end{Bmatrix} . \tag{32}$$

Since matrices $\mathbf{L}_X$ are condensation operators, their application on the sub-matrices in Eq. (32) increases the efficiency in solving the linear systems in Eq. (26). In fact, terms $\mathbf{D}_{II}^{'-1}\mathbf{D}'_{IX}$ in Eq. (26) can be evaluated directly in Eq. (32) as $\mathbf{D}_{II}^{'-1}\left(\mathbf{D}'_{IX}\mathbf{L}_X^H\right)$ so involving the solution of two liner systems for a significantly lower number of columns. Such a shrewdness ensures great efficiency for unit cells with several internal DOFs. Finally, the problem can be rearranged in the form

$$\begin{bmatrix} -\mathbf{C}_{TB}^{-1}\mathbf{C}_{TT} & \mathbf{C}_{TB}^{-1} \\ \mathbf{C}_{BT} - \mathbf{C}_{BB}\mathbf{C}_{TB}^{-1}\mathbf{C}_{TT} & \mathbf{C}_{BB}\mathbf{C}_{TB}^{-1} \end{bmatrix} \begin{Bmatrix} \hat{\mathbf{q}}_T \\ \hat{\mathbf{e}}_T \end{Bmatrix} = \mathbf{T}'(\omega,\theta,\alpha) \begin{Bmatrix} \hat{\mathbf{q}}_T \\ \hat{\mathbf{e}}_T \end{Bmatrix} = \begin{Bmatrix} \hat{\mathbf{q}}_B \\ \hat{\mathbf{e}}_B \end{Bmatrix} , \tag{33}$$

where $\mathbf{T}'(\omega,\theta,\alpha)$ is the transfer matrix of the layer related to the original variables for a specific incident plane wave.

3.3. Choice of interface variables

The final step in the procedure represented in Fig. 2 involves manipulation of the resulting transfer matrix, $\mathbf{T}'(\omega,\theta,\alpha)$, taking into account the requested variables at its interfaces. Only three kind of interfaces are allowed by the present model: solid, fluid and mixed. The TMM variables usually chosen

to describe the acoustic field in these interfaces are collected in the following vectors

$$\mathbf{V}_{\text{fluid}} = [\ p\ ,\ v_z^f\ ]^T\ , \tag{34}$$

$$\mathbf{V}_{\text{solid}} = [\ v_{x'}\ ,\ v_z\ ,\ \sigma_{zz}\ ,\ \sigma_{zx'}\ ]^T\ , \tag{35}$$

$$\mathbf{V}_{\text{mixed}} = [\ v_{x'}\ ,\ v_z\ ,\ v_z^f\ ,\ \sigma_{zz}\ ,\ \sigma_{zx'}\ ,\ p\ \ ]^T\ . \tag{36}$$

It should be noted that when the bottom and top interfaces are of a different nature, we obtain a rectangular transfer matrix; see the periodic structure on the right side of Fig. 4. For fluid or mixed interfaces the fluid velocity at the boundaries can be expressed as

$$v_z^f = \pm \frac{e_f}{i\omega\rho_f A}\ , \tag{37}$$

where the total area of the unit cell, $A = L_x L_y$, is involved. The term is positive for the bottom surface and negative at the opposite one, since positive displacement at the bottom boundary increases pressure and consequently fluid energy.

First, we show how to manipulate the original transfer matrix for a layer with both fluid interfaces. The quantities collected in the vector $\mathbf{V}_{\text{fluid}}$ can be expressed in terms of generalized variables, for the bottom and top surfaces, in the following way

$$\begin{aligned} \mathbf{V}_B &= [\ \hat{p}_B\ ,\ \hat{e}_{Bf}/(i\omega\rho_f A)\ ]^T \\ \mathbf{V}_T &= [\ \hat{p}_T\ ,\ -\hat{e}_{Tf}/(i\omega\rho_f A)\ ]^T\ . \end{aligned} \tag{38}$$

The final transfer matrix in Eq. (2) therefore becomes

$$\mathbf{T} = \begin{bmatrix} 1 & 0 \\ 0 & 1/(i\omega\rho_f A) \end{bmatrix} \mathbf{T}' \begin{bmatrix} 1 & 0 \\ 0 & -i\omega\rho_f A \end{bmatrix}\ . \tag{39}$$

We now manipulate the original transfer matrix for a layer with both solid interfaces. The quantities collected in the vector $\mathbf{V}_{\text{solid}}$ can be expressed in terms of generalized variables, for the bottom and top surfaces, in the following way

$$\begin{aligned}
\mathbf{V}_B &= [\ i\omega(C\hat{q}_{Bx} + S\hat{q}_{By})\ ,\ i\omega\hat{q}_{Bz}\ ,\ -\hat{e}_{Bz}/A\ ,\ -(C\hat{e}_{Bx} + S\hat{e}_{By})/A\ ]^T \\
\mathbf{V}_T &= [\ i\omega(C\hat{q}_{Tx} + S\hat{q}_{Ty})\ ,\ i\omega\hat{q}_{Tz}\ ,\ \hat{e}_{Tz}/A\ ,\ (C\hat{e}_{Tx} + S\hat{e}_{Ty})/A\ ]^T
\end{aligned} \tag{40}$$

where $C = \cos(\alpha)$ and $S = \sin(\alpha)$. So, the final transfer matrix in Eq. (2) appears as

$$\mathbf{T} = \begin{bmatrix} i\omega\mathbf{E} & \mathbf{0} \\ \mathbf{0} & -\mathbf{F}/A \end{bmatrix} \mathbf{T}' \begin{bmatrix} \mathbf{E}^T/(i\omega) & \mathbf{0} \\ \mathbf{0} & A\mathbf{F}^T \end{bmatrix}\ , \tag{41}$$

where

$$\mathbf{E} = \begin{bmatrix} C & S & 0 \\ 0 & 0 & 1 \end{bmatrix}\ ,\ \mathbf{F} = \begin{bmatrix} 0 & 0 & 1 \\ C & S & 0 \end{bmatrix}\ . \tag{42}$$

Finally, the transfer matrix for a layer with both mixed interfaces is derived. The quantities collected in the vector $\mathbf{V}_{\text{mixed}}$ can be expressed in terms of generalized variables, for the bottom and top surfaces, as follows

$$\begin{aligned}
\mathbf{V}_B &= [\ i\omega(C\hat{q}_{Bx} + S\hat{q}_{By})\ ,\ i\omega\hat{q}_{Bz},\ \hat{e}_{Bf}/(i\omega\rho_f A)\ ,\ -\hat{e}_{Bz}/A\ ,\ -(C\hat{e}_{Bx} + S\hat{e}_{By})/A\ ,\ \hat{p}_B\ ]^T \\
\mathbf{V}_T &= [\ i\omega(C\hat{q}_{Tx} + S\hat{q}_{Ty})\ ,\ i\omega\hat{q}_{Tz}\ ,\ -\hat{e}_{Tf}/(i\omega\rho_f A)\ ,\ \hat{e}_{Tz}/A\ ,\ (C\hat{e}_{Tx} + S\hat{e}_{Ty})/A\ ,\ \hat{p}_T\ ]^T
\end{aligned} \tag{43}$$

The final transfer matrix thus becomes

$$\mathbf{T} = \begin{bmatrix} i\omega\hat{\mathbf{E}} & \mathbf{G}/(i\omega\rho_f A) \\ \mathbf{G} & -\hat{\mathbf{F}}/A \end{bmatrix} \mathbf{T}' \begin{bmatrix} \hat{\mathbf{E}}^T/(i\omega) & \mathbf{G}^T \\ -i\omega\rho_f A\mathbf{G}^T & A\hat{\mathbf{F}}^T \end{bmatrix} \tag{44}$$

where

$$\hat{\mathbf{E}} = \begin{bmatrix} C & S & 0 & 0 \\ 0 & 0 & 1 & 0 \\ 0 & 0 & 0 & 0 \end{bmatrix}\ ,\ \hat{\mathbf{F}} = \begin{bmatrix} 0 & 0 & 1 & 0 \\ C & S & 0 & 0 \\ 0 & 0 & 0 & 0 \end{bmatrix}\ ,\ \mathbf{G} = \begin{bmatrix} 0 & 0 & 0 & 0 \\ 0 & 0 & 0 & 0 \\ 0 & 0 & 0 & 1 \end{bmatrix}\ . \tag{45}$$

The transfer matrix of a layer characterized by in-plane periodicity has been derived on the basis of a FE model of its unit cell. The matrix obtained fully defines the layer in a TMM context and can also describe a sequence of a finite number of identical sub-layers by means of Eq. (12).

4. Applications

The procedure presented above has been integrated in a homemade TMM code, also implementing the analytical formulations of layers of different types and handling various kinds of stratification. To verify the effectiveness of the proposed procedure, the media accounted for will be interposed between two semi-infinite fluids with $\rho = 1.25$ kg m^{-3} and $c = 343.6$ m s^{-1} and results will be compared in terms of the Transmission Loss (TL) in diffusive field with $0 \leq \theta \leq \pi/2$ in Eq. (11). A mesh convergence study is presented only for the first application. In the following applications only the results related to the discretization that satisfactorily balances accuracy and computing resources for the frequency range explored are reported.

4.1. Uniform plate

The first application is intended to prove the effectiveness of the solid interfaces condition, Eq. (41). It concerns a 10 mm thick aluminum alloy (E=72 GPa, ν= 0.3, ρ= 2800 kg m^{-3}) plate. The periodic unit is a brick as thick as the plate. It has been modeled with elements of first and second order. In-plane dimensions and discretization of the unit cell have been proven to have no effect on the results. The panel may be modeled with n hexahedron elements (hexa for short) through the thickness. Alternatively, it may be divided into n identical sub-layers, each modeled with a single hexa: transfer

matrices are evaluated for a single sub-layer and global transfer matrices are derived by means of Eq. (12). The two approaches provide the very same results while the second one significantly decreases the computational burden. The results of the proposed procedure have been compared with those obtained through the analytical model of the solid layer. Fig. 6 shows the TL factors obtained with 8-node and 20-node hexas. It is clear that the number of 8-node sub-cells strongly affects the solution while the calculation with a single 20-node sub-cell reaches the analytical solution in the frequency range explored. The description of the shear and longitudinal waves involved in the acoustic transmission improves as long as the number of hexas through the thickness grows and the error decreases according to the FE order. However, the number of sub-cells does not significantly affect the computational cost, since Eq. (12) is exploited. This simple application proves the effectiveness of the method developed for layers with solid interfaces.

4.2. Unidirectional fiber-reinforced composite

The second application involves a thin composite plate whose equivalent mechanical properties have been derived in [33] by means of FE analysis and the rule of mixtures (ROM). They have been here used with analytical 3D elasticity theory [27] to predict sound transmission. The mechanical properties of the basic materials are presented in Table 1 while the two selected equivalent material models are listed in Table 2. The plate is 1.5 mm tick unidirectional fiber-reinforced composite with a 50% fiber volume fraction and a 7.6 μm fiber diameter. The medium comprises 157 identical layers each containing a single row of fibers. Each layer is modeled with the sub-cell depicted in Fig. 7 the sizes of which are $9.5252\times9.5252\times0.7938$ μm^3.

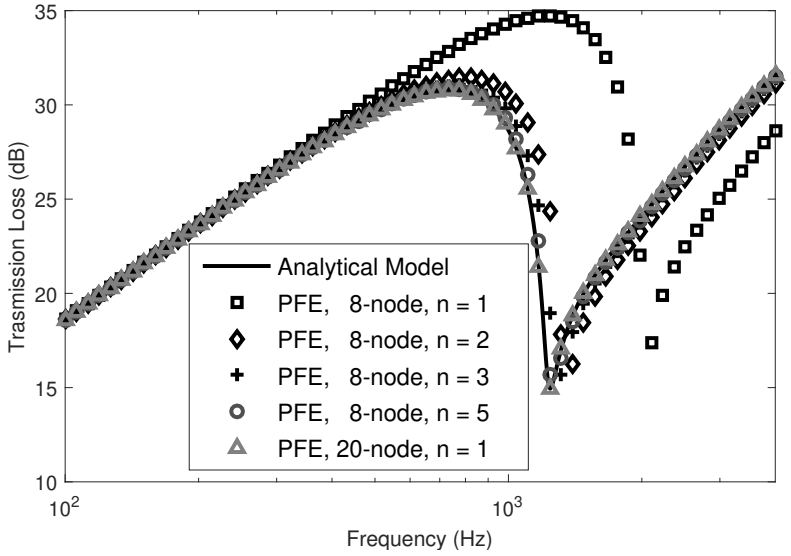

Figure 6: Transmission loss in a diffuse field for an aluminum plate modeled with 8-node hexas

The FE model of the unit cell is made of 8-node hexas and the properties of the matrix and the fiber are listed in Table 1 [33] where the fiber direction, k, corresponds to the y axis of Fig. 7. It is not truly representative of the actual arrangement of fibers, but it is not expected to affect the results because of the high ratio of wavelength over fiber diameter. The results shown in Fig. 8 prove the effectiveness of both the homogenization techniques in the frequency range explored. In the frame of the acoustic prediction the simplifications typical of the rule of mixtures are not relevant and sophisticated homogenization techniques are not able to improve the model accuracy. Because of the typical values of fiber diameters, discrepancies between the periodic FE approach and equivalent homogeneous models are expected only at very high frequencies. Nevertheless, at high frequencies, the diffusive in-

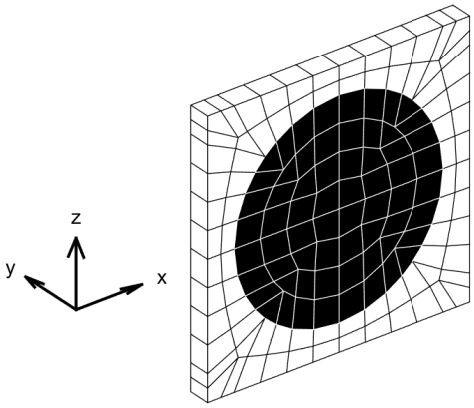

Figure 7: FE model of a cell for an unidirectional fiber-reinforced composite, fibers (black) and matrix (white)

put field could become non-representative, and the related integration has a high computational cost, regardless of the way in which transfer matrices are obtained. For these reasons, higher frequencies have not been explored.

Material	E(GPa)	G(GPa)	ν	ρ(kg m^{-3})
T300 Carbon Fiber k	230	8.96	0.20	1810
T300 Carbon Fiber $\perp$	13.75	4.83	0.25	1810
Amorphous Carbon Matrix	62.21	26.62	0.30	2000

Table 1: Properties of the materials used (k is the fiber direction)

	E_k	$E_\perp$	$G_{k\perp}$	$G_{\perp\perp}$	$\nu_{k\perp}$	$\nu_{\perp\perp}$	$\nu_{\perp k}$	ρ(kg m^{-3})
FEM	147.43	36.11	18.04	16.03	0.275	0.262	0.067	1905
ROM	149.61	30.50	15.60	15.72	0.250	0.275	0.067	1905

Table 2: Properties of the unidirectional fiber-reinforced composite (k is the fiber direction, elastic moduli are expressed in GPa)

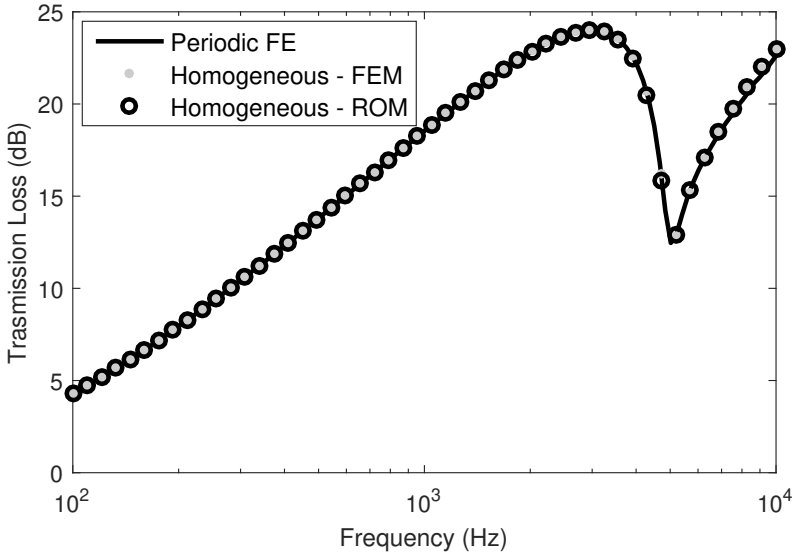

Figure 8: Transmission loss in a diffuse field for an unidirectional fiber-reinforced composite ($\alpha = \pi/2$)

4.3. Sandwich panel with honeycomb core

The third application is intended to prove the effectiveness of the mixed interfaces condition, Eq. (44). It concerns a sandwich panel with a honeycomb core. Both the core and the skins are made of aluminum alloy (E=72 GPa, ν= 0.3, ρ= 2800 kg m^{-3}). The skins are 0.5 mm thick and all the honeycomb faces have 0.1 mm thickness. Two kinds of core have been considered, hexagonal and auxetic. The hexagonal cells have a side of 10 mm and the auxetic cells have a short side of 10 mm and a long side of 20 mm. Both cells are 20 mm tall. Fig. 9 shows the in-plane geometry of the unit cells for both core types. A three-node triangular element combining a Discrete Kirchhoff Triangle (DKT) bending element and a Constant Strain Triangle (CST) membrane element has been used to model the honeycomb faces and skins. A

four-node tetrahedral element has been used to model the acoustic cavities in the honeycomb core. The panel has been modeled entirely with the proposed procedure using the unit cells depicted in Fig. 10. Alternatively the structure can be considered as layered: the total transfer matrix can be evaluated for a specific incident plane wave as $\mathbf{T}_{\text{skin}} \cdot \mathbf{T}^4_{\text{core}/4} \cdot \mathbf{T}_{\text{skin}}$, where $\mathbf{T}_{\text{skin}}$ is the transfer matrix of the skin, involving the analytical formulation of a solid layer, and $\mathbf{T}_{\text{core}/4}$ is the transfer matrix obtained with the proposed procedure for the FE model restricted to the gray elements in Fig. 10. The latter approach is the one preferred since it provides accurate results and significantly decreases the computational burden. Usually, in vibro-acoustic applications, the honeycomb core of a sandwich panel is modeled as an equivalent homogeneous medium in order to exploit TMM capabilities. The in-plane and out-of-plane equivalent mechanical properties of the honeycomb can be expressed in terms of cell geometry and of the thickness of the faces [34]. Fig. 11 shows the TL obtained through the proposed procedure (PFE), along with the analytical calculation performed with the equivalent models (EM) of the honeycomb cores. The presence of fluid in the honeycomb cavities has marginal effects on acoustic transmission. The results demonstrate the effectiveness of the equivalent model for the honeycomb core in the frequency range explored.

4.4. Double-leaf wall with internal structural links

The last application is intended to prove the effectiveness of the proposed procedure for large heterogeneity scales. It concerns a double-leaf wall with structural links between them. Two plates are linked by longitudinal vertical septums. Both the plates and the septums are made of aluminum alloy (E=72 GPa, ν= 0.3, ρ= 2800 kg m^{-3}). Referring to Fig. 12, $T_S = T_W =$

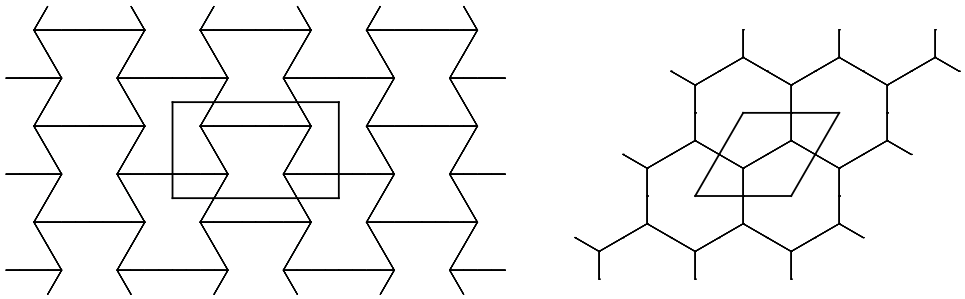

Figure 9: Minimal unit cell for the auxetic (left) and hexagonal (right) honeycomb core

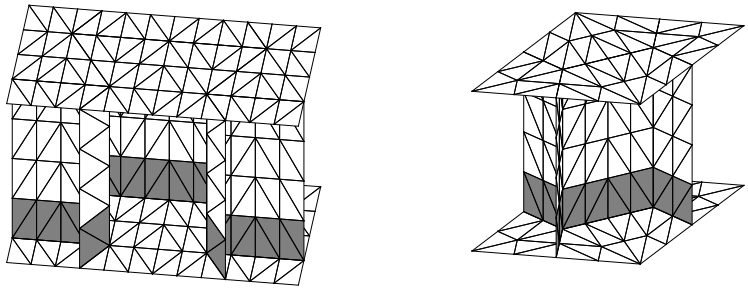

Figure 10: Cell structural grid for the auxetic (left) and hexagonal (right) honeycomb core

1 mm, $S = 100$ mm and $H = 10$ mm. The three-node triangular element described above has been used to model both the plates and the septums. Four-node tetrahedral elements have been used to model the acoustic cavities. Fig. 13 shows the structural mesh. Double panel structures filled with air or absorbent fiberglass can be found in a wide range of applications and were therefore extensively studied in the literature. A recent article by Hongisto [35] provides a detailed comparison of the prevalent models for prediction of sound transmission through such constructions. Of the 20 models presented, only a few are able to deal with connections between panels. In these models, the problem is addressed by decoupling total transmission in terms of

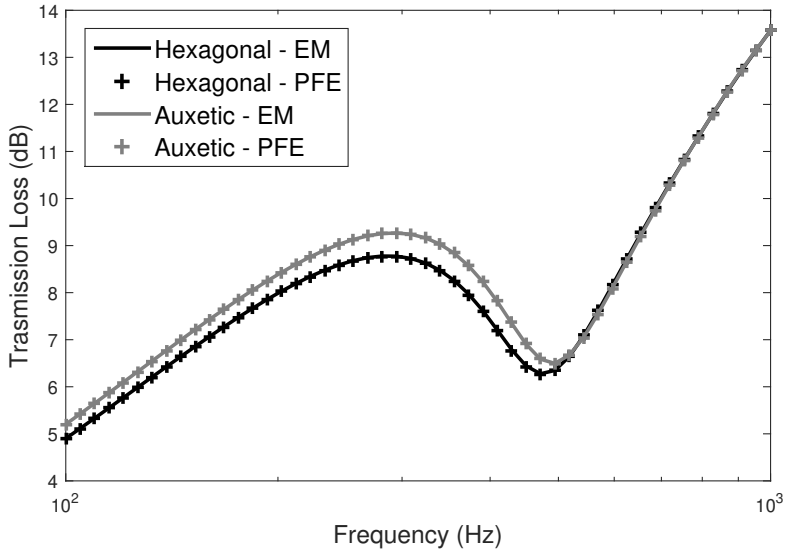

Figure 11: Transmission loss in a diffuse field for a sandwich panel with a honeycomb core ($\alpha = 90$)

a fluid-borne path through the cavity and a structure-borne path through the connectors. Fig. 14 shows the TL obtained with the proposed procedure along with the results provided by Davy's model [36] which is declared in [35] as the most accurate in terms of predicted sound transmission. Again, the presence of fluid in the cavities has marginal effects on acoustic transmission. The results prove the effectiveness of Davy's model in the frequency range explored, except in the coincidence region. In that application, because of the large heterogeneity scale of the structure in relation to the frequency range explored, the proposed procedure reveals its greater ability to handle local dynamics with respect to equivalent homogeneous models such as Davy's.

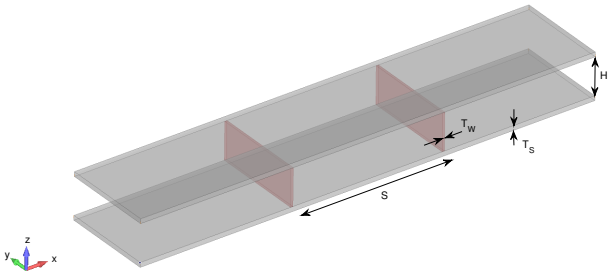

Figure 12: Portion of a double-leaf wall with structural links

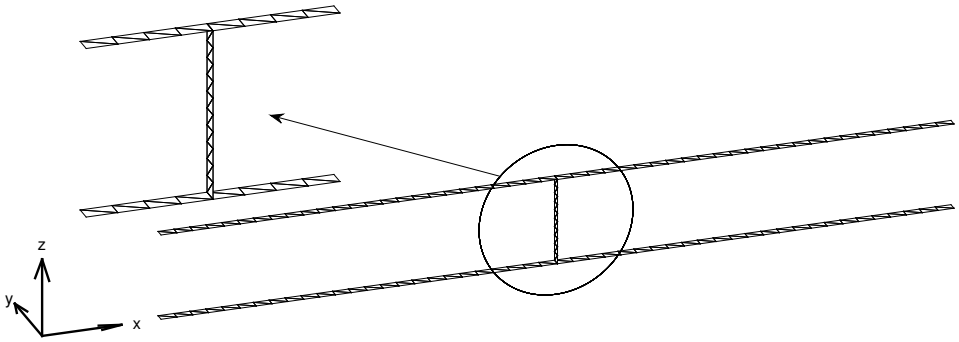

Figure 13: Cell structural mesh for a double-leaf wall with structural links with a detail of the connection region

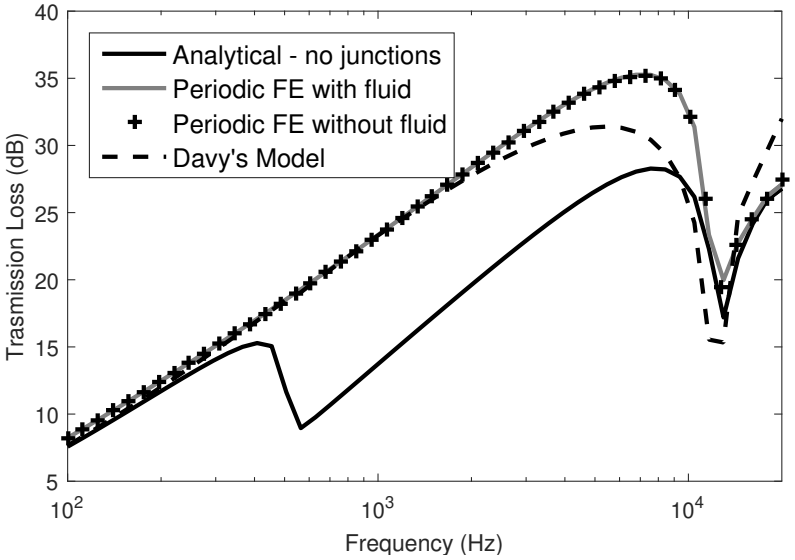

Figure 14: Transmission loss in a diffuse field for a double-leaf wall with structural links ($\alpha = 0$)

5. Conclusions

A general procedure for obtaining the acoustic transfer matrix of a planar periodic medium is described. The procedure involves manipulating the dynamic stiffness matrix of the FE model related to the unit cell: the wave approach is applied to the unit cell, and a further projection based on the trace of the incident wave leads to the transfer matrix of the medium. The matrix thus obtained is used in a TMM context to predict sound transmission through the medium. The proposed procedure preserves the local dynamics involved in the acoustic transmission through the medium, preventing the problem of dealing with dispersion curves and SEA models. Moreove, it allows to exploit the versatility of the TMM and makes it easy to deal with anisotropic and heterogeneous media in a TMM context, avoiding the need

for homogeneous equivalent models and overcoming their limitations.

The accuracy of the model in predicting sound transmission loss has been verified through agreement with the analytical formulation of a homogeneous plate. Applications to non-homogeneous media make it possible to assess the accuracy of the corresponding simplified, equivalent models. The FE model can be related to the whole thickness of the structure, in this case the transfer matrix obtained does not need further manipulations. In case of different layers with the same nature, the TMM allows to build the complete model by simply multiplying individual matrices. In case of layers with different nature, adequate interface relations are available in the frame of TMM. The computational effort related to the proposed procedure depends on the FE model size. In homogeneous media, it appears only slightly higher with respect to that of the analytical procedure: they may be modeled with a few finite elements by exploiting the ability to model only a portion of the thickness and by recovering the overall transfer matrix as a power of the elementary one.

Ultimately, the proposed procedure, combined with TMM, could represent an effective acoustic tool in a FE analysis environment, due to its versatility and efficiency.

References

[1] C. P. Smolenski, E. M. Krokosky, Dilational-mode sound transmission in sandwich panels, The Journal of the Acoustical Society of America 54 (6) (1973) 1449–1457. doi:http://dx.doi.org/10.1121/1.1914444.

[2] Numerical prediction of sound transmission through finite mul-

tilayer systems with poroelastic materials, The Journal of the Acoustical Society of America 100 (1) (1996) 346–354. doi:http://dx.doi.org/10.1121/1.415956.

[3] J. Ramakrishnan, L. Koval, A finite element model for sound transmission through laminated composite plates, Journal of Sound and Vibration 112 (3) (1987) 433 – 446. doi:http://dx.doi.org/10.1016/S0022-460X(87)80109-8.

[4] A. Arjunan, C. Wang, K. Yahiaoui, D. Mynors, T. Morgan, M. English, Finite element acoustic analysis of a steel stud based double-leaf wall, Building and Environment 67 (0) (2013) 202 – 210. doi:http://dx.doi.org/10.1016/j.buildenv.2013.05.021.

[5] A. Arjunan, C. Wang, K. Yahiaoui, D. Mynors, T. Morgan, V. Nguyen, M. English, Development of a 3d finite element acoustic model to predict the sound reduction index of stud based double-leaf walls, Journal of Sound and Vibration 333 (23) (2014) 6140 – 6155. doi:http://dx.doi.org/10.1016/j.jsv.2014.06.032.

[6] F. C. Sgard, N. Atalla, J. Nicolas, A numerical model for the low frequency diffuse field sound transmission loss of double-wall sound barriers with elastic porous linings, The Journal of the Acoustical Society of America 108 (6) (2000) 2865–2872. doi:http://dx.doi.org/10.1121/1.1322022.

[7] Lyon, R. H., DeJong, R. G., Theory and Application of SEA, Butterworth, London, 1995.

[8] R. J. M. Craik, Sound Transmission Through Buildings using Statistical Energy Analysis, Gower press, London, 1996.

[9] S. Finnveden, Evaluation of modal density and group velocity by a finite element method, Journal of Sound and Vibration 273 (12) (2004) 51 – 75. doi:http://dx.doi.org/10.1016/j.jsv.2003.04.004.

[10] S. Ghinet, N. Atalla, H. Osman, The transmission loss of curved laminates and sandwich composite panels, The Journal of the Acoustical Society of America 118 (2) (2005) 774–790. doi:http://dx.doi.org/10.1121/1.1932212.

[11] B. R. Mace, E. Manconi, Modelling wave propagation in two-dimensional structures using finite element analysis, Journal of Sound and Vibration 318 (45) (2008) 884 – 902. doi:http://dx.doi.org/10.1016/j.jsv.2008.04.039.

[12] E. Manconi, B. R. Mace, R. Garziera, The loss-factor of pre-stressed laminated curved panels and cylinders using a wave and finite element method, Journal of Sound and Vibration 332 (7) (2013) 1704 – 1711. doi:http://dx.doi.org/10.1016/j.jsv.2012.09.039.

[13] V. Cotoni, R. Langley, P. Shorter, A statistical energy analysis subsystem formulation using finite element and periodic structure theory, Journal of Sound and Vibration 318 (45) (2008) 1077 – 1108. doi:http://dx.doi.org/10.1016/j.jsv.2008.04.058.

[14] D. Chronopoulos, M. Ichchou, B. Troclet, O. Bareille, Computing the broadband vibroacoustic response of arbitrarily thick layered panels by

a wave finite element approach, Applied Acoustics 77 (2014) 89 – 98. doi:http://dx.doi.org/10.1016/j.apacoust.2013.10.002.

[15] L. Brillouin, Wave Propagation in Periodic Structures: Electric Filters and Crystal Lattices, Dover, 1946.

[16] Cremer, L., Heckl, M., Zur theorie der biegekettenleiter, Archiv der elektrischen Ubertragung 7 (1953) 261–270.

[17] M. A. Heckl, Investigations on the vibrations of grillages and other simple beam structures, The Journal of the Acoustical Society of America 36 (7) (1964) 1335–1343. doi:http://dx.doi.org/10.1121/1.1919206.

[18] D. J. Mead, The random vibrations of a multi-supported heavily damped beam, Shock and Vibration Bulletin 35 (1966) 45–54.

[19] D. J. Mead, Free wave propagation in periodically supported, infinite beams, Journal of Sound and Vibration 11 (1970) 181–197.

[20] D. Mead, A general theory of harmonic wave propagation in linear periodic systems with multiple coupling, Journal of Sound and Vibration 27 (2) (1973) 235 – 260. doi:http://dx.doi.org/10.1016/0022-460X(73)90064-3.

[21] A. L. Abrahamson, Flexural wave mechanics - An analytical approach to the vibration of periodic structures forced by convected pressure fields, Journal of Sound Vibration 28 (1973) 247–258. doi:10.1016/S0022-460X(73)80105-1.

[22] R. M. Orris, M. Petyt, A finite element study of harmonic wave propagation in periodic structures, Journal of Sound and Vibration 33 (2) (1974) 223 – 236. doi:http://dx.doi.org/10.1016/S0022-460X(74)80108-2.

[23] R. M. Orris, M. Petyt, Random response of periodic structures by a finite element technique, Journal of Sound and Vibration 43 (1) (1975) 1 – 8. doi:http://dx.doi.org/10.1016/0022-460X(75)90199-6.

[24] Allard, J. F., Atalla, N., Propagation of Sound in Porous Media: Modelling Sound Absorbing Materials - Second Edition, John Wiley and Sons, Ltd, 2009.

[25] M. Villot, C. Guigou, L. Gagliardini, Predicting the acoustical radiation of finite size multilayered structures by applying spatial windowing on infinite structures, Journal of Sound and Vibration 245 (3) (2001) 433 – 455. doi:http://dx.doi.org/10.1006/jsvi.2001.3592.

[26] F. G. Leppington, K. H. Heron, E. G. Broadbent, Resonant and non-resonant transmission of random noise through complex plates, Proceedings: Mathematical, Physical and Engineering Sciences 458 (2019) (2002) pp. 683–704. doi:http://dx.doi.org/10.1098/rspa.2001.0870.

[27] C. Huang, S. Nutt, Sound transmission prediction by 3-d elasticity theory, Applied Acoustics 70 (5) (2009) 730 – 736. doi:http://dx.doi.org/10.1016/j.apacoust.2008.09.003.

[28] N. Chandra, S. Raja, K. N. Gopal, Vibro-acoustic response and sound transmission loss analysis of functionally graded plates,

Journal of Sound and Vibration 333 (22) (2014) 5786 – 5802. doi:http://dx.doi.org/10.1016/j.jsv.2014.06.031.

[29] N. Tolosana, M. Carrera, R. G. de Villoria, L. Castejon, A. Miravete, Numerical analysis of three-dimensional braided composite by means of geometrical modeling based on machine emulation, Mechanics of Advanced Materials and Structures 19 (1-3) (2012) 207–215. doi:http://dx.doi.org/10.1080/15376494.2011.578784.

[30] S. Green, M. Matveev, A. Long, D. Ivanov, S. Hallett, Mechanical modelling of 3d woven composites considering realistic unit cell geometry, Composite Structures 118 (0) (2014) 284 – 293. doi:http://dx.doi.org/10.1016/j.compstruct.2014.07.005.

[31] X. Zeng, L. P. Brown, A. Endruweit, M. Matveev, A. C. Long, Geometrical modelling of 3d woven reinforcements for polymer composites: Prediction of fabric permeability and composite mechanical properties, Composites Part A: Applied Science and Manufacturing 56 (0) (2014) 150 – 160. doi:http://dx.doi.org/10.1016/j.compositesa.2013.10.004.

[32] Fahy, F., Gordonio, P., Sound and Structural Vibration: Radiation, Transmission and Response - Second Edition, Academic Press, 2007.

[33] M. Blacklock, D. R. Hayhurst, Initial elastic properties of unidirectional ceramic matrix composite fiber tows, Journal of Applied Mechanics 79 (5) (2012) 1–11. doi:http://dx.doi.org/10.1115/1.4005585.

[34] L. J. Gibson, M. F. Ashby, Cellular Solids: structure properties - Second Edition, Cambridge University Press, 1997.

[35] V. Hongisto, Sound insulation of double panels - comparison of existing prediction models, Acta Acustica united with Acustica 92 (1) (2006) 61–78.

[36] J. L. Davy, Sound transmission of cavity walls due to structure borne transmission via point and line connectionsa, The Journal of the Acoustical Society of America 132 (2) (2012) 814–821. doi:http://dx.doi.org/10.1121/1.4733533.